SPH simulation for seismic behavior of earth structures

Y. Ono[1], S. Nishida[2] and J. Kiyono[3]

[1] *Assistant Professor, Dept. of Urban Management , Kyoto University, Kyoto, Japan*
[2] *Graduate Student, Dept. of Urban Management , Kyoto University, Kyoto, Japan*
[3] *Associate Professor, Dept. of Urban Management, Kyoto University, Kyoto, Japan*
Email: ysk@mbox.kudpc.kyoto-u.ac.jp, shingo@quake2.kuciv.kyoto-u.ac.jp, kiyono@quake.kuciv.kyoto-u.ac.jp

ABSTRACT :

The earthquake response analysis of earth structures using the Smoothed Particle Hydrodynamics (SPH) was introduced in this paper. We showed that the corrective smoothed particle method (CSPM), which is a modified version of the conventional SPH, could achieve higher accuracy than the conventional SPH for earthquake response analysis. To illustrate this, three numerical simulations were carried out; the one dimensional elastic wave propagation problem with reflection, the earthquake response analysis of the one dimensional elastic soil and the two-dimensional elasto-plastic soil. Finally, we demonstrated the SPH simulation of the collapse behavior of an earth structure.

KEYWORDS: smoothed particle hydrodynamics, corrective smoothed particle method, earth structure and earthquake response analysis

1. INTRODUCTION

Strong ground motion causes large deformation with tension cracks and slip failure to earth structures. The finite element analysis is widely used to simulate the earthquake damage of earth structures. However, it is difficult to estimate residual displacement precisely because the FE analysis hardly simulates behavior of earth structures after discontinuity such as sliding or tension crack have taken place. In the present paper, the Smoothed Particle Hydrodynamics (SPH) is examined to simulate dynamic behavior of earth structures excited by strong ground motion. One advantage of the SPH method the FE analysis is that the SPH could handle discontinuity destruction in a continuum body. The SPH was invented by Lucy (1977) and Gingold and Monaghan (1977) for dealing with a compressive fluid body. Since 1990s, the SPH has been applied to solid body dynamics(Randles and Libersky,1996 and Gray et al.,2001).

The objective of this paper is to present the earthquake response analysis of earth structures. In the first section, the fundamental equations of the SPH are introduced. Also, the corrective Smoothing Particle Method (CSPM) which achieves higher accuracy than the SPH is described. In the second section, several numerical tests are conducted to illustrate the capability of the SPH and the CSPM.

2.SMOOTHED PARTICLE HYDRODYNAMICS

2.1 Conventional SPH

The SPH is one kind of interpolation theory and it consists of two interpolation techniques, i.e., kernel approximation and particle approximation. The kernel approximation begins with the following equation.

$$f(\mathbf{x}) = \int_{\Omega} f(\mathbf{x}')\delta(\mathbf{x}-\mathbf{x}')d\mathbf{x}' \tag{2.1}$$

where $f(\mathbf{x})$ is a function of the three-dimensional position vector $\mathbf{x}$ and $\delta(\mathbf{x}-\mathbf{x}')$ is the Dirac delta function. Ω is the domain where the function $f(\mathbf{x})$ is defined. Replacing the delta function $\delta(\mathbf{x}-\mathbf{x}')$ in (2.1) by a function $W(\mathbf{x}-\mathbf{x}',h)$, we get

$$\langle f(\mathbf{x})\rangle = \int_{\Omega} f(\mathbf{x}')W(\mathbf{x}-\mathbf{x}',h)d\mathbf{x}' \tag{2.2}$$

where $W(\mathbf{x}-\mathbf{x}',h)$ is called a kernel function or smoothing function. The angle bracket means the kernel approximation operator. h is a parameter which defines the influence area of the kernel function $W(\mathbf{x}-\mathbf{x}',h)$. Although many types of kernel functions have been proposed, the cubic B-spline kernel function, which is proposed by Monaghan and Lattanzio(1985), is most preferred in many SPH literatures because of its computational efficiency. The cubic B-spline kernel function is,

$$W(R,h) = \alpha_d \times \begin{cases} \frac{2}{3} - R^2 + \frac{1}{2}R^3 & 0 \le R < 1 \\ \frac{1}{6}(2-R)^3 & 1 \le R < 2 \\ 0 & R \ge 2 \end{cases} \tag{2.3}$$

where $R = \frac{|\mathbf{x}-\mathbf{x}'|}{h}$ and for one-, two- and three-dimensional, $\alpha_d = 1/h$, $15/7\pi h^2$ and $3/2\pi h^3$, respectively. In the present study we also use the cubic B-spline kernel function.

In the SPH method, the integral representation of the equation (2,2), is converted to a summation over a set of discrete particles. The particle approximation for a function $f(\mathbf{x})$ at particle i is,

$$f_i = \sum_{j=1}^{N} \frac{m_j}{\rho_j} f_j W(\mathbf{x}_i - \mathbf{x}_j, h) \tag{2.4}$$

where N is the total number of particles in the influence domain of particle i as shown in Figure 1. m_j and ρ_j is the mass and density associated to particle j, respectively.

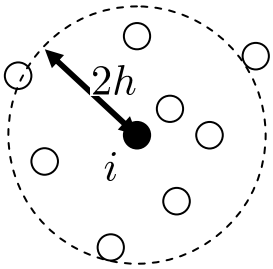

Figure 1 SPH particles neighboring particle j

In most engineering problems, the first derivative of a function $f(\mathbf{x})$ is often required rather than the function $f(\mathbf{x})$ itself. Instead of direct application of equation (2.4) to the first derivative of a function $f(\mathbf{x})$, the following form is commonly used.

$$\nabla \cdot f_i = \sum_{j=1}^{N} \frac{m_j}{\rho_j}(f_i - f_j)\nabla W(\mathbf{x}_i - \mathbf{x}_j, h) \tag{2.5}$$

The SPH method has been applied successfully to various continuous mechanics problems. However, two big problems which can cause inaccuracy are known. First, the kernel approximation, equation (2.2) used cannot reproduce the function itself completely. In other words, the SPH does not satisfy even the zero order consistency. Second, near or on a boundary, the integral (or summation) is truncated due to particle deficiency and the SPH approximation becomes inaccurate. Therefore, Chen et al. proposed the corrective smoothed particle method (CSPM) which can eliminate these problems successfully. The CSPM formulation is briefly introduced in the next section.

2.2 The Corrective Smoothed Particle Method(CSPM)

Chen et al.(1999) proposed the following form of the kernel approximation instead of equation (2.2).

$$\langle f(\mathbf{x})\rangle = \frac{\int_{\Omega} f(\mathbf{x}')W(\mathbf{x}-\mathbf{x}',h)d\mathbf{x}'}{\int_{\Omega} W(\mathbf{x}-\mathbf{x}',h)d\mathbf{x}'} \tag{2.6}$$

The denominator of equation (2.6) is called the corrective term and if it is equal to 1, equation (2.6) becomes identical to equation (2.2). The particle approximation form of equation (2.6) can be written by

$$f_i = \frac{\sum_{j=1}^{N} \frac{m_j}{\rho_j} f_j W(\mathbf{x}_i - \mathbf{x}_j, h)}{\sum_{j=1}^{N} \frac{m_j}{\rho_j} W(\mathbf{x}_i - \mathbf{x}_j, h)} \tag{2.7}$$

The first derivatives for particle *i* can be obtained by the following simultaneous equations.

$$A_i^{\beta\alpha} f_i^{,\alpha} = F_i^{\beta} \tag{2.8}$$

where

$$A_i^{\beta\alpha} = \sum_{j=1}^{N} \frac{m_j}{\rho_j} (x_j^{\alpha} - x_i^{\alpha}) W_{ij}^{,\beta} \tag{2.9}$$

$$F_i^{\beta} = \sum_{j=1}^{N} \frac{m_j}{\rho_j} (f_j - f_i) W_{ij}^{,\beta} \tag{2.10}$$

The indices α and β denote spatial components and the superscript $,\alpha$ indicates the first derivative for spatial component α and $W_{ij} = W(x_i - x_j, h)$. Note that the CSPM satisfy the zero and first order consistency conditions completely. The effectiveness of the CSPM for earthquake response analysis is demonstrated in the following section.

3. RESULTS AND DISCUSSIONS

3.1 Case 1: 1D Elastic Wave Propagation

To show the accuracy of the SPH method, elastic wave propagation in one dimensional bar (uniaxial strain problem) is studied here. As shown in Figure 1, we fix the left end of the bar rigidly and stress $\sigma(t)$ is applied to the right hand end. Young's modulus E and the density ρ is assumed to be 100N/m^2 and 1000kg/m^3, respectively. The length of the bar is set to 4.0m. The governing equations of this problem are given by

$$\frac{\partial v(x,t)}{\partial t} = \frac{1}{\rho}\frac{\partial \sigma(x,t)}{\partial x} \tag{3.1}$$

$$\dot{\sigma}(x,t) = E\frac{\partial v(x,t)}{\partial x} \tag{3.2}$$

in which v is velocity at position x. For the boundary treatment, a particle is centered on a boundary and boundary values are assigned explicitly. The explicit Euler scheme is employed for time integration. Although the SPH is a pure Lagrangian method, all particles are spatially fixed here. The particles are arranged with equal interval 0.02m. Therefore, total 201 particles are used. The Finite Difference Method (FDM) is also conducted for comparison.

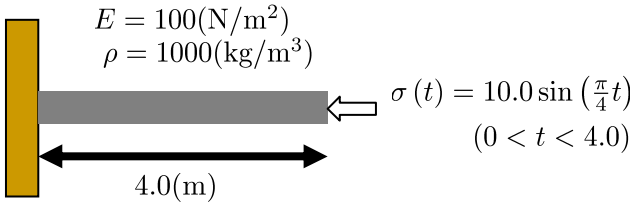

Figure 2 1D Elastic Wave Propagation Test

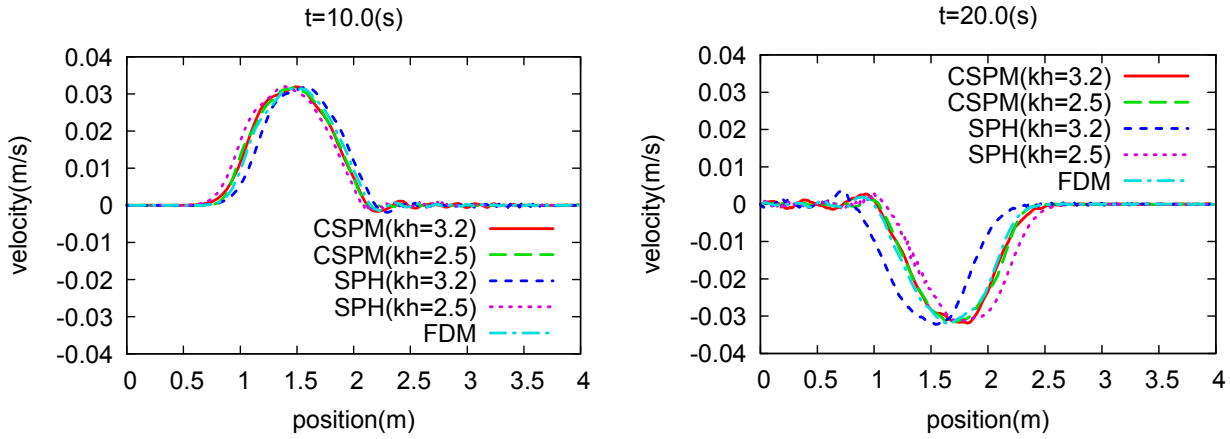

Figure 3 Velocity distribution at t=10.0s (LHS) and t=20.0s (RHS)

Figure 3 shows the snapshots of the velocity distribution along the bar. In Figure 3, kh indicates the ratio of the smoothing length to the particle spacing. At t=10.0(s) the wave front has not reached at the left end and the wave has reflected once at the left end between 10.0(s) and 20.0(s). Two different values of the smoothing length are examined for the conventional SPH and the CSPM. The results from the CSPM agree very well with those from the FDM independently on the smoothing length while the SPH results less accuracy and the wave speed is affected by the smoothing length. This problem of the conventional SPH is caused by the lack of the first order consistency.

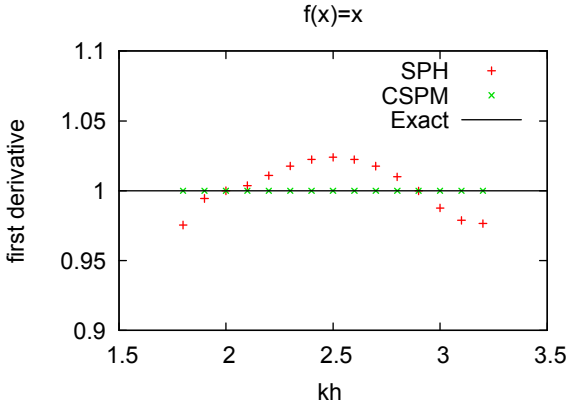

Figure 4 Variation of the estimated first derivative

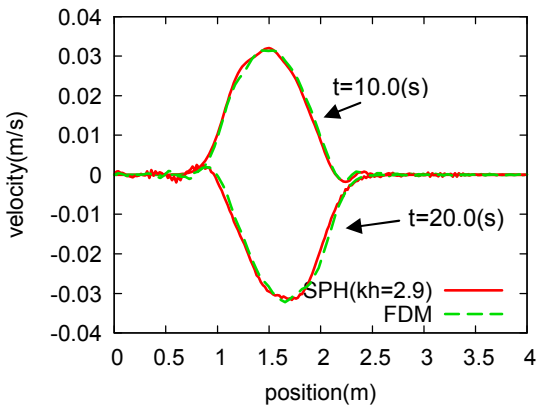

Figure 5 Velocity distribution with the SPH (kh=2.9dp)

In Figure 4 the first derivatives of the function $f(x)=x$ calculated by the conventional SPH and the CSPM are plotted. The horizontal axis corresponds to the smoothing length ratio to the particle spacing. Here all particles are arranged with equal interval. The smoothing length does not affect the accuracy of the CSPM while the accuracy of the conventional SPH changes. Figure 4 suggests that the SPH can give the best approximation when kh is equal to 2.0 or 2.9. It is confirmed in Figure 5 where the conventional SPH with kh=2.9 shows good agreement with the FDM.

3.2 Case 2: 1D Earthquake Response Analysis of Elastic Soil Model

The response of one-dimensional elastic soil column model to earthquake excitation is analyzed here. The soil

model conducted is shown in Figure 4. The governing equation is written by

$$\frac{\partial v(x,t)}{\partial t} = \frac{1}{\rho}\frac{\partial \sigma(x,t)}{\partial x} + a(t) \tag{3.3}$$

$$\dot{\sigma}(x,t) = G\frac{\partial v(x,t)}{\partial x} \tag{3.4}$$

in which $a(t)$ is acceleration of the input ground motion and G is shear modulus. Figure 5 shows the input ground motion used here. The density ρ and Poisson's ratio ν is set to be 2000kg/m^3 and 0.40 for all layers respectively. The finite element method (FEM) is also conducted for comparison.

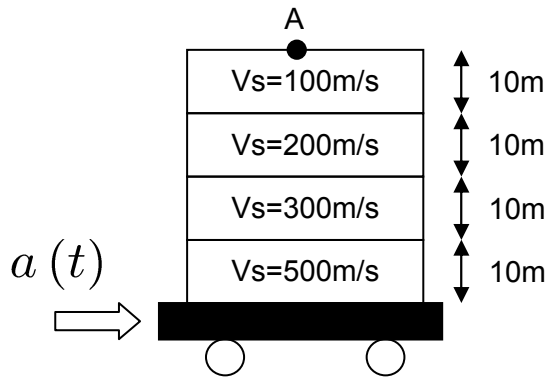

Figure 6 1D Soil column model

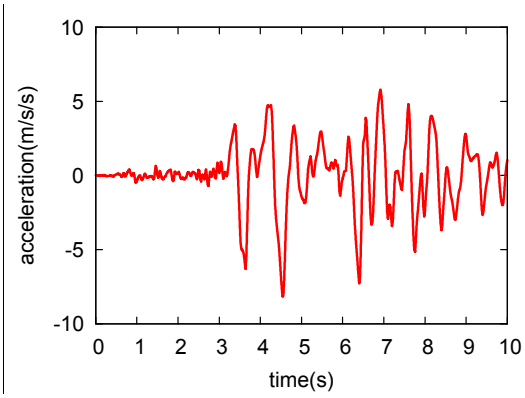

Figure 7 The input ground motion (JMA Kobe 1995)

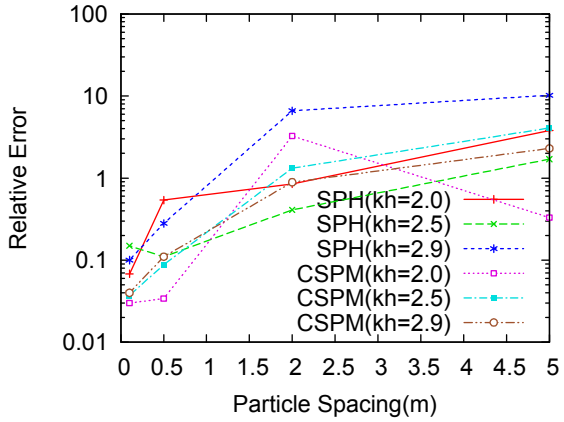

Figure 8 Variation of the relative error η (Case 2)

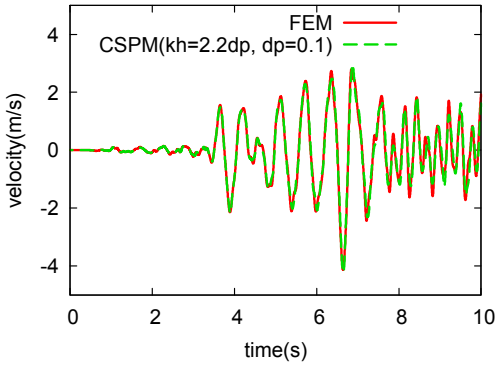

Figure 9 The time history at Point A by CSPM

We ran 18 simulations using this soil model with the particle spacing dp=0.1,0.5,2.0,5.0(m) and the smoothing length kh=2.0dp, 2.5dp, 2.9dp for the conventional SPH and the CSPM. To discuss the accuracy of each model we define the relative error η by

$$\eta = \frac{\int_0^T \left| v^{FEM} - v^{SPH} \right|^2 dt}{\int_0^T \left| v^{FEM} \right|^2 dt} \tag{3.5}$$

in which $v^{FEM}(t)$ is the velocity given by the FEM and $v^{SPH}(t)$ is by the conventional SPH or the CSPM. T is the duration of the analysis. The result is summarized in Figure 8. One can conclude from results depicted in Figure 8 that the CSPM achieves higher accuracy than the conventional SPH when the particle spacing is small. The highest accuracy is obtained by the CSPM with kh=2.0dp and dp=0.1(m). The time history at the ground

surface (Point A in Figure 6) is plotted in Figure 9 and compared to the result from the FEM.

3.3 Case 3: 2D Earthquake Response Analysis of Elasto-Plastic Soil Model

In this example the two dimensional soil model is analyzed by the conventional SPH and the CSPM. The soil model which is 20m wide and 10m height (see Figure 10) is excited by the acceleration shown in Figure 9. The plain strain is assumed. The bottom boundary particles are fixed. For the boundary particles on the both side, the vertical displacement is fixed to be zero while the horizontal one is free. Stress free condition is explicitly given to the free-surface boundary particles. The viscous damping term cv is added to the RHS of equation (3.3) where c is the damping coefficient and set to be 0.2 here. The elasto-plastic model with the Mohr-Coulomb yield surface and the associated flow rule is employed. The internal friction angle and the cohesion coefficient are set to be 30(deg.) and 120(kN/m^2), respectively. The shear wave velocity, the density and Poisson's ratio are 100(m/s), 1900(kg/m^3) and 0.40.

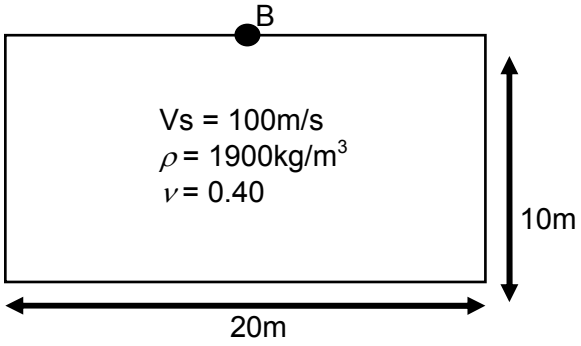

Figure 10 Two dimensional ground model

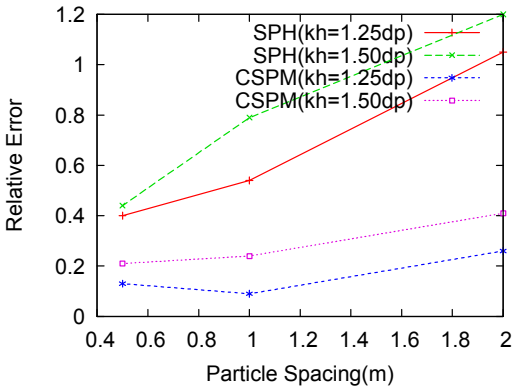

Figure 11 Variation of the relative error η (Case 3)

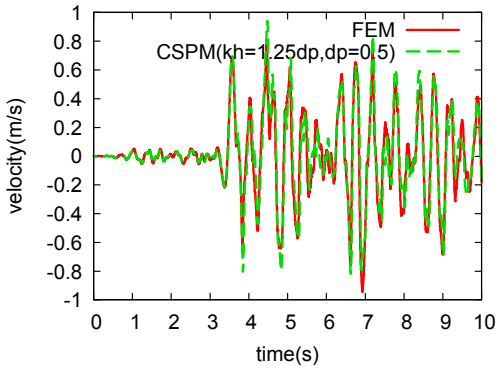

Figure 12 Time history of response at Point B

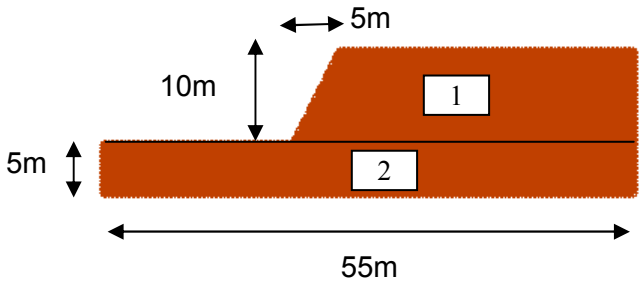

Figure 13 Earth structure model

Figure 11 shows the variation of the relative error η computed by equation (3.5) with the particle spacing dp and the smoothing length kh. It is clear that the CSPM gives better results than the conventional SPH. Figure 12 compares the time histories of the response at Point B shown in Figure 10 computed by the CSPM (dp=0.5m, kh=1.25dp) with that of the FEM.

3.4 Case 4: 2D Collapse Simulation of Earth structure

The earth structure model depicted in Figure 13 is excited by the acceleration shown in Figure 9. The shear wave velocity is 200m/s for the domain 1 and 400m/s for the domain 2. The density and Poisson's ratio are given to be 1900kg/m^3 and 0.35 respectively for the entire model. The boundary particles on the both sides of the domain 2 and the right-hand-side of the domain 1 are constrained as well as the particles on the bottom edge

of the domain 2. The free stress condition is directly assigned to the other boundary particles. In this case the Lagrangian approach is employed, namely the particle arrangement is updated at every time step and the kernel functions are rebuild. The Jaumann stress rate tensor is used for the finite rotation effect. The same constitutive relationship as the previous example is used except that the cohesion coefficient c and the internal friction angle ϕ are dropped after yielding. Here we use c=60(kN/m^2), ϕ=20.0(deg.) before yielding and c=30(kN/m^2), ϕ=10.0(deg.) for post-yielding. Total 10105 particles are used and they are regularly distributed with 0.25m interval at the initial time step. Figure 13 shows the snapshots of the deformation of the earth structure. At t=4.0s, one can see that the shear failure band was developed and the slip began. At t=8.0s, the slip failure took place and a few gaps appeared on the top of the earth structure.

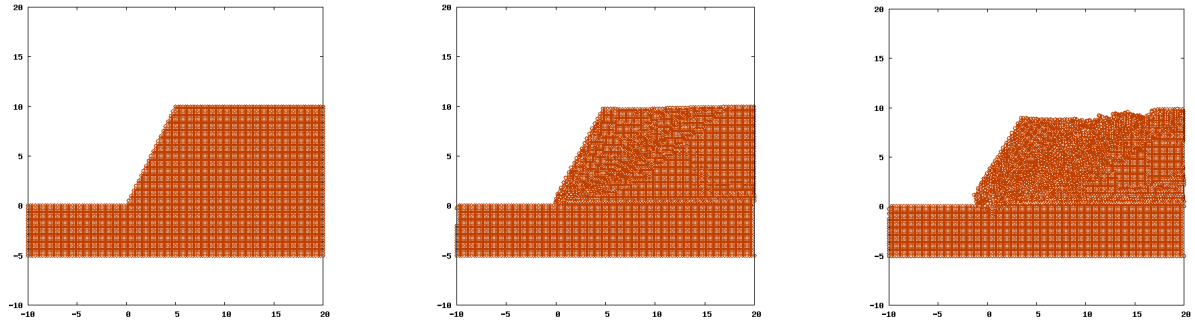

(a) 0.0s (b) 4.0s (c) 8.0s

Figure 13 The deformation of the earth structure model excited by the earthquake ground motion (computed by the CSPM)

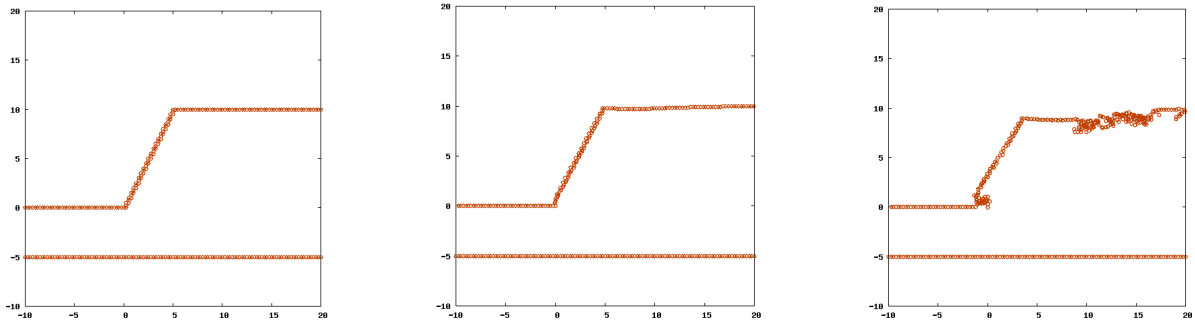

(a) 0.0s (b) 4.0s (c) 8.0s

Figure 14 The captured boundary particles

When the deformation of the model becomes large under the seismic excitation, new boundary particles may appear due to cracks or collapse. These new boundary particles must be captured at every time step. In order to identify the boundary particles we used the criteria which is defined by

$$\left|\Psi_i\right| \geq \varepsilon \tag{3.6}$$

where

$$\Psi_i = -\sum_{i=1}^{N} \frac{m_j}{\rho_j} \nabla W_{ij} \tag{3.7}$$

Note that Ψ_i corresponds to the outward normal vector at the particle i when the particle i locates on the boundary. If the particle i is far from the boundary and surrounded by other particles enough, Ψ_i becomes zero. We determine ε=0.5 by trial and error for this case. Figure 14 shows that the boundary particles are captured properly.

4. CONCLUSIONS

We discussed the capability of the SPH and the CSPM, which is one modification of the SPH, for earthquake response analysis of soil with a series of the numerical simulations. We showed that the CSPM could give better results for earthquake response analysis of soil than the conventional SPH. Also we showed that the SPH can be used to simulate collapse behavior of earth structures.

REFERENCES

Lucy, L.B. (1977). A numerical approach to the testing of the fission hypothesis. *Astronical Journal* **82**, 1013-1020.
Gingold, R.A. and Monaghan J.J. (1977) Smoothed particle hydrodynamics: Theory and application to non-spherical stars. *Monthly Notices for the Royal Astronomical Society* **181**, 375-389.
Randles, P.W. and Libersky, L.D. (1996). Smoothed Particle Hydrodynamics: Some recent improvements and applications. *Computer Methods in Applied Mechanics and Engineering* **139**, 375-408.
Gray, J.P., Monaghan J.J. and Swift, R.P. (2001) SPH elastic dynamics. *Computer Methods in Applied Mechanics and Engineering* **190**, 6641-6662.
Monaghan, J.J. and Lattanzio, J.C. (1985) A refined particle method for astrophysical problems, *Astronomy and Astrophysics* **149**, 135-143.
Chen, J.K., Beraun, J.E. and Jih, C.J. (1999) Completeness of corrective smoothed particle method for linear elastodynamics. *Computational Mechanics* **24**, 273-285.